Available online at www.sciencedirect.com
ScienceDirect
Journal of the European Ceramic Society 29 (2009) 245–253
www.elsevier.com/locate/jeurceramsoc

Layered mixed-anion compounds: Epitaxial growth, active function exploration, and device application

Hidenori Hiramatsu [a,*], Yoichi Kamihara [a], Hiroshi Yanagi [b], Kazushige Ueda [a,c], Toshio Kamiya [a,b], Masahiro Hirano [a,d], Hideo Hosono [a,b,d]

[a] *Exploratory Research for Advanced Technology–Solution-Orientated Research for Science and Technology (ERATO–SORST), Japan Science and Technology Agency (JST) in Frontier Research Center, Tokyo Institute of Technology, Mail-box S2-13, 4259 Nagatsuta-cho, Midori-ku, Yokohama 226-8503, Japan*
[b] *Materials and Structures Laboratory, Tokyo Institute of Technology, Mail-box R3-1, 4259 Nagatsuta-cho, Midori-ku, Yokohama 226-8503, Japan*
[c] *Department of Materials Science, Faculty of Engineering, Kyushu Institute of Technology, 1-1 Sensui-cho, Tobata-ku, Kitakyushu 804-8550, Japan*
[d] *Frontier Research Center, Tokyo Institute of Technology, Mail-box S2-13, 4259 Nagatsuta-cho, Midori-ku, Yokohama 226-8503, Japan*

Available online 2 May 2008

Abstract

Optoelectronic properties and device applications of layered mixed-anion compounds such as oxychalcogenide LaCuO*Ch* (*Ch* = chalcogen) and oxypnictide LaT_MO*Pn* (T_M = 3d transition metal, *Pn* = pnicogen) are reviewed. Several distinctive functions have been found in these materials based on our original material exploration concept. Fabrication of high-quality epitaxial films of LaCuO*Ch* leads to clarifying the excellent electrical and optical properties such as high hole mobility of 8 $cm^2/(V\,s)$ and heavy hole doping at $>10^{21}$ cm^{-3} in LaCuOSe, and sharp and tunable-wavelength photoluminescence in the solid–solution systems in LaCuO*Ch*. In addition, a room temperature operation of a light-emitting diode is demonstrated using LaCuOSe as a light-emitting layer. These results suggest that the layered oxychalcogenides have potential for light-emitting layers as well as transparent hole-injection layers in organic/inorganic light-emitting diodes. Furthermore, by extending the material system from the copper-based oxychalcogenides to isostructural compounds, transition metal-based oxypnictides LaT_MOP (T_M = Fe, Ni), we have found novel superconductors, LaFeOP and LaNiOP.

Keywords: Epitaxial thin films; Solid state reaction; Electrical properties; Optical properties; Superconductivity

1. Introduction

Recently, it is recognized that wide gap oxide-based semiconductors are attractive materials for short wavelength optoelectronic devices. However, p-type doping is much difficult than n-type doping for wide gap oxide-based semiconductors because the valence band maximum (VBM) of a typical oxide is formed by rather deep oxygen $2p^6$ orbitals. Among a number of wide gap oxide-based materials, we found that layered oxychalcogenides, LaCuO*Ch* (*Ch* = chalcogen such as S, Se, and Te), are wide gap p-type semiconductors[1–3] by extending our material design concept for wide gap p-type oxide semiconductors.[4–6] The design concept proposes that the hybridization between Cu 3d orbitals and chalcogen *n*p (*n*: principal quantum number, $n \geq 3$) orbitals enhances delocalization of positive holes at the valence band maximum and improve the hole mobility. Fig. 1(a) shows the crystal structure of LaCuO*Ch*. This material consists of alternate stacking of (LaO) and (Cu*Ch*) layers along the *c*-axis.[7–12] The energy band structure is of a direct-transition type, and the conduction band minimum (CBM) is primarily composed of Cu 4s, and the VBM are mainly composed of well-hybridized band of Cu 3d and chalcogen *n*p as expected above.[13–18] That is, the components of the VBM electronic states meets the above design concept, and it is clarified that the (Cu*Ch*) layers work as carrier transport layers.

Furthermore, this kind of the layered structure may be, in a sense, regarded as a kind of superlattice composed of wide gap (LaO) (*cf.* the energy gap of the simple oxide La_2O_3 is ~5.5 eV) oxide layers and narrow gap (Cu*Ch*) (*cf.* that of Cu_2Ch is <2 eV) chalcogenide layers. If there is a large band offset between these layers, a tunneling barrier formed by the (LaO) layers may be high enough to confine the wave function of the holes in the chalcogenide layers, and the superlattice may also be regarded as multiple quantum wells. Therefore we expect these

* Corresponding author. Tel.: +81 45 924 5128; fax: +81 45 924 5127.
E-mail address: h-hirama@lucid.msl.titech.ac.jp (H. Hiramatsu).

0955-2219/$ – see front matter © 2008 Elsevier Ltd. All rights reserved.
doi:10.1016/j.jeurceramsoc.2008.03.016

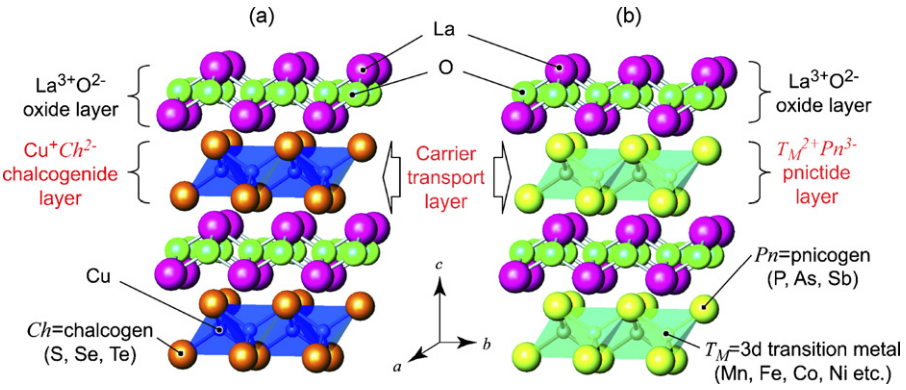

Fig. 1. Crystal structures of layered mixed-anion compounds. Lattice system: tetragonal, space group: *P*4/*nmm* (No. 129). (a) Oxychalcogenide LaCuO*Ch* (*Ch* = chalcogen). (b) Oxypnictide LaT_MO*Pn* (T_M = divalent 3d transition metal, *Pn* = pnicogen). (Cu*Ch*) and (T_M*Pn*) layers, which work as carrier transport layers, are composed of edge-sharing networks of CuCh_4 and $T_M Pn_4$ tetrahedra, respectively. Four out of the six edges of a tetrahedron are shared with neighboring tetrahedra.

materials exhibit unique electrical and optical properties originating from the naturally formed, two-dimensional structure. Actually, the two-dimensional structure[19] leads to interesting optical properties in LaCuO*Ch*. For instance, ultraviolet–blue photoluminescence (PL)[2,3,20] and large third order optical nonlinearity[21] that originate from room-temperature stable excitons are observed. Thus, this material series can be a promising candidate for an active layer in light-emitting diodes (LEDs) that operate in the ultraviolet–blue region as well as transparent hole-injection electrodes.

In order to explore other unique materials, we have extended the materials system to isostructural oxypnictides, LaT_MO*Pn* (T_M = 3d transition metals, *Pn* = pnicogens such as P, As, and Sb). Since Cu^+ ions in LaCuO*Ch* are replaced by divalent 3d transition metal ions in LaT_MO*Pn* and divalent Ch^{2-} anion by trivalent Pn^{3-} anions as shown in Fig. 1(b),[22–25] we expect that the (T_M*Pn*) layer governs the carrier transport like the (Cu*Ch*) layer in the oxychalcogenides, and that novel properties due to spins in the T_M ions such as ferromagnetism and superconductivity may be found in the oxypnictides.

In this paper, we review the unique optoelectronic properties that have been recently found in the high-quality epitaxial thin films of the oxychalcogenides such as a high hole mobility, heavy hole doping over 10^{21} cm^{-3}, a highly efficient light-emission. The successful fabrication of high-quality epilayer led to a first demonstration of room-temperature operation of a hetero pn junction LED based on LaCuOSe. Further, superconducting properties of LaT_MOP (T_M = Fe and Ni) are also reviewed.

2. Oxychalcogenide, LaCuO*Ch* (*Ch* = chalcogen)

2.1. Heteroepitaxial growth[26,27]

It is not easy to fabricate high-quality samples of LaCuO*Ch* because LaCuO*Ch* have somewhat complex chemical compositions and the chalcogenide components easily evaporate from a sample at high temperatures especially in vacuum. Although we had made extensive efforts to grow epitaxial films by a high temperature pulsed laser deposition (PLD) technique, epitaxial films had not been obtained. Therefore, we employed a reactive solid-phase epitaxy (R-SPE) technique,[28] which was first invented for fabricating single-crystalline films of homologous series layered compounds, $InGaO_3(ZnO)_m$ (m = integer). Currently, this process has been applied to fabrication of high-quality epitaxial films of many multi-component compounds.[29–42] The heteroepitaxial films of LaCuO*Ch* were successfully grown when a thin Cu layer was used as a sacrificial layer.

Fig. 2 shows a flow chart of the R-SPE process used to grow LaCuO*Ch* [*Ch* = $S_{1-x}Se_x$ (x = 0–1)] epitaxial films. A PLD technique was applied for the film deposition using a metallic Cu and single-phase LaCuO*Ch* (*Ch* = S and Se) ceramics as targets. First, a thin Cu (~5 nm) layer was deposited on a MgO (0 0 1) substrate at 400 °C. Then, an amorphous bi-layer of LaCuOSe/LaCuOS was deposited on the Cu (~5 nm)/MgO structure. The anion composition (x) is controllable by tuning the thickness ratio of the LaCuOSe and LaCuOS layers. The resulting multi-layered film, capped with an YSZ plate, was sealed in an evacuated SiO_2 glass ampule (<0.2 Pa) with a small amount of powders of respective materials, and then the evacuated ampule was thermally annealed at 1000 °C. The capping with the YSZ plate and the addition of the powders in the ampule are crucial for maintaining the stoichiometric composition in the annealed films. The Cu layer firstly deposited is a key to obtaining the epitaxial films in this process. In order to grow epitaxial films, it is inevitable that the thin Cu layer has a discontinuous structure with triple junctions of the Cu film, the amorphous LaCuO*Ch* layer, and the substrate,[43] where the triple junctions create epitaxial seed grains during the post-thermal annealing. The resulting seed grains work as a template for subsequent solid-phase epitaxial growth of the amorphous LaCuO*Ch* layer from the substrate–film interface to the film's top surface.

Fig. 3 shows a cross-sectional transmission electron microscope (TEM) image of a LaCuOS epitaxial film prepared by R-SPE. A layered structure originating from the parallel stacking of LaCuOS (0 0 *l*) planes is clearly observed over the entire area. The film–substrate interface is sharp without other compounds such as reaction sub-products and/or residual Cu. The thin Cu layer deposited in the R-SPE process completely disappears due to the solid-state reaction with the amorphous LaCuOS layer.

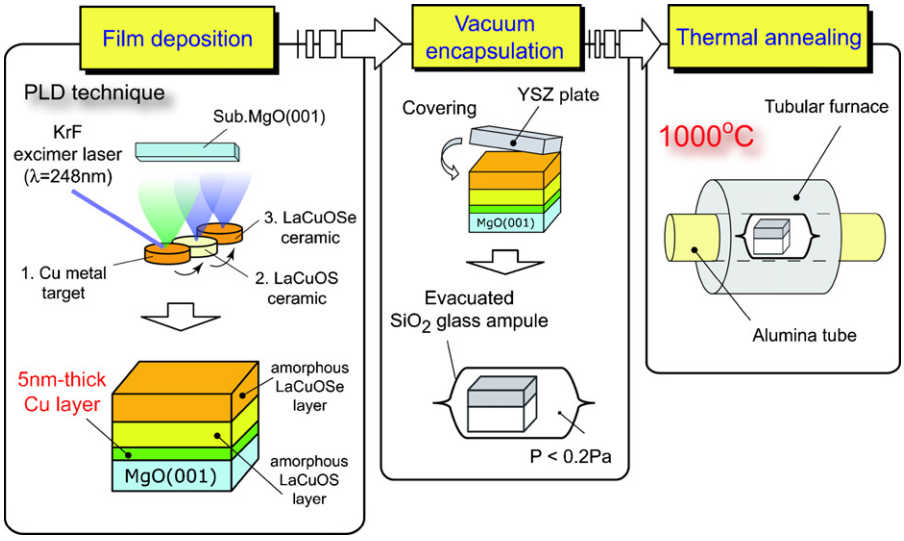

Fig. 2. Process flow of R-SPE for heteroepitaxial growth of $LaCuOS_{1-x}Se_x$ ($x = 0$–1).

Although phase mismatches between the crystalline lattices in the film and the substrate, which would result from the large lattice mismatch between LaCuOS and MgO (~5%), are observed at the hetero-interface, the lattice structure in the film appears to be relaxed within a few atomic layers from the interface without propagating dislocations.

Four-axes high-resolution X-ray diffraction measurements also revealed that all LaCuO*Ch* films prepared by R-SPE are heteroepitaxially grown on MgO (0 0 1) substrates, keeping the crystallographic orientation of (0 0 1)[1 1 0] LaCuO*Ch* || (0 0 1)[1 1 0] MgO. The lattice parameters of the LaCuO*Ch* epitaxial films are close to those of powders, demonstrating that the crystalline lattices in the films are fully relaxed and have little distortion. These results verify that the obtained films are of high-quality and R-SPE is a practical technique for the heteroepitaxial growth of the layered oxychalcogenides, LaCuO*Ch*.

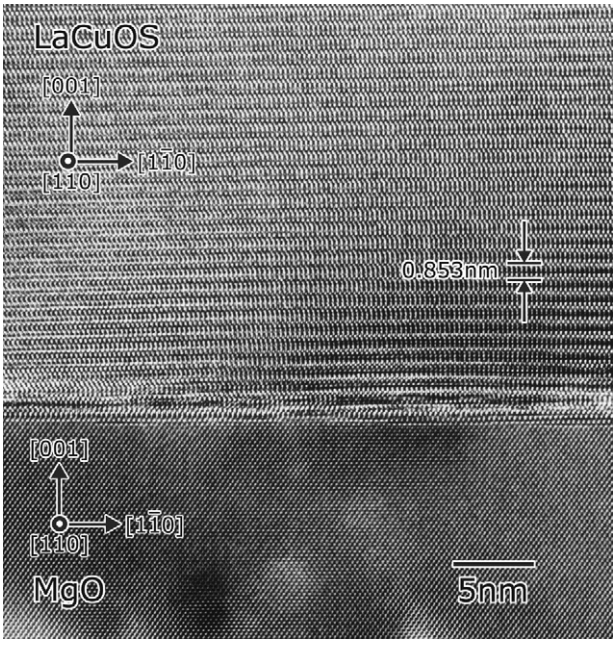

Fig. 3. Cross-sectional TEM image of LaCuOS epitaxial film on MgO (0 0 1) substrate prepared by R-SPE.

2.2. *Carrier transport properties of $LaCuOS_{1-x}Se_x$ ($x = 0$–1) epitaxial films*[44,45]

Fig. 4 shows the carrier transport properties of undoped $LaCuOS_{1-x}Se_x$ ($x = 0$–1) epitaxial films at 300 K. The Seebeck coefficients were positive for all the films. This result, along with phase angles = ~0° obtained by ac-Hall measurements, verifies that all the films are p-type conductors. The Se addition monotonously increases the electrical conductivity (σ, circles) and Hall mobility (μ, triangles). Since the carrier concentration (n, squares) remains almost constant irrespective of change in the Se content, the increase in the conductivity originates from the enhanced hole mobility. A model, in which the hole conduction paths are broadened by orbital-hybridization enhanced by replacing the chalcogen ion from S to Se, explains this result well. That is, the Se addition increases hole mobility due to the enhanced covalency and hybridization between Se 4p and Cu

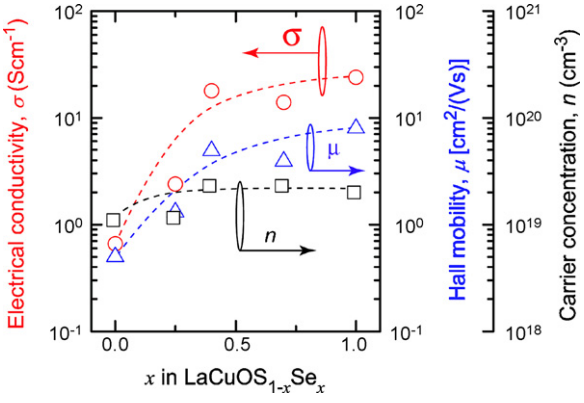

Fig. 4. Carrier transport properties of undoped $LaCuOS_{1-x}Se_x$ ($x = 0$–1) epitaxial films measured at 300 K as a function of Se content x.

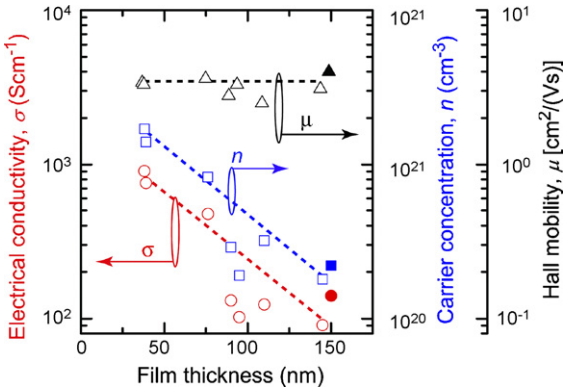

Fig. 5. Film thickness dependence of carrier transport properties of LaCuOSe:Mg epitaxial films measured at room temperature. Closed symbols show the data reported previously in Ref. [44].

3d orbitals at the VBM. The Hall mobility at 300 K obtained in undoped LaCuOSe reaches 8.0 $cm^2/(V\,s)$, which is comparable to that of a wide gap p-type III–V semiconductor GaN:Mg [$\sim$10 $cm^2/(V\,s)$].[46–48] This result is consistent with the materials design concept and our aim described in the introduction. Thus, modifying the anionic species is an effective way to modulate the VBM dispersion to design a new wide gap p-type semiconductor.

2.3. Heavy hole doping over 10^{21} cm^{-3} of LaCuOSe epitaxial films[49]

To further increase the p-type conductivity of oxychalcogenides, alkaline-earth metal ions such as Sr^{2+}, Ca^{2+}, and Mg^{2+} were added to LaCuOSe epitaxial films, because LaCuOSe has the highest mobility among the oxychalcogenides. Among these additives, only the Mg^{2+} addition changed the LaCuOSe epitaxial film with 150 nm thickness to a degenerate p-type semiconductor with a high carrier concentration of $\sim 2 \times 10^{20}$ cm^{-3} by keeping a moderately large hole mobility $\sim$4 $cm^2/(V\,s)$, which is the first demonstration of high-density hole doping at $>10^{20}$ cm^{-3} in a wide gap p-type epitaxial film.[44] Furthermore, we have recently found that one order of magnitude higher density hole doping (1.7×10^{21} cm^{-3}) is achieved in thinner ($\sim$40 nm) LaCuOSe:Mg epitaxial films.

Fig. 5 shows the film thickness dependence of carrier transport properties of the LaCuOSe:Mg epitaxial films. Although a constant Hall mobility $\sim$3.5 $cm^2/(V\,s)$ is maintained, the carrier concentration increases as the film thickness decreases, and finally reaches the hole concentration of 1.7×10^{21} cm^{-3} and the electrical conductivity of 910 S cm^{-1} for 40-nm-thick films. Due to the high-density hole, the transport properties showed a degenerate conduction. These σ and n values are nearly an order of magnitude larger than those previously reported for 150-nm-thick films in Ref. [44]. Typically, it is difficult to achieve such a high-density hole doping for wide gap p-type semiconductors such as GaN:Mg[48] and ZnO:N[50] due to the deep acceptor levels, which are $\sim$100–200 meV deep from the VBM. This is the first demonstration of high-density hole doping $>10^{21}$ cm^{-3} in a wide gap p-type semiconductor epilayer.

Atomic force microscopy (AFM) showed that the film surfaces of the LaCuO*Ch* films consisted of tetragonally faceted

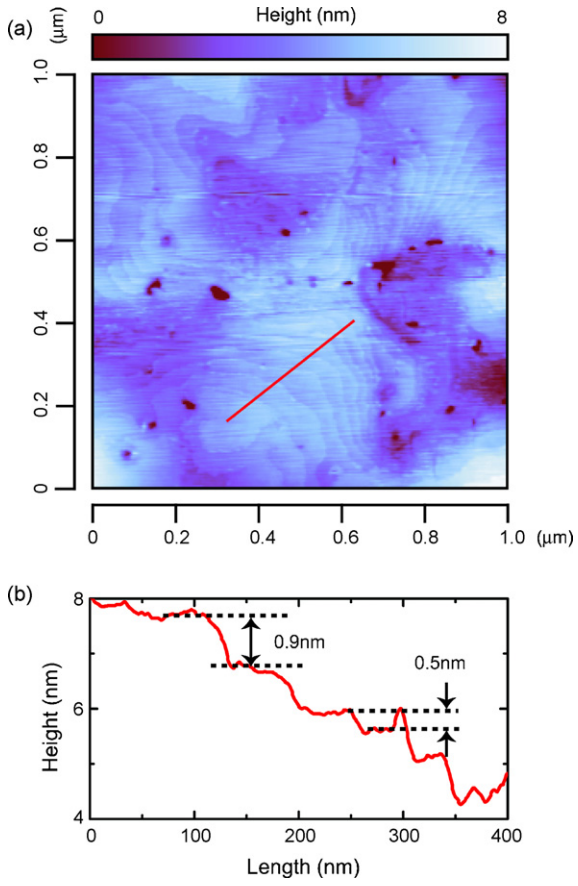

Fig. 6. (a) AFM image of CMP-polished, LaCuOSe:Mg epitaxial film with 40 nm thickness. (b) Cross-sectional profile along the line in (a).

grains and have somewhat large roughness.[32,51] By employing chemical mechanical polishing (CMP), an atomically flat, terrace, and step surface was obtained in the 40-nm-thick high hole density films as shown in Fig. 6(a). The step heights are $\sim$0.9 and $\sim$0.5 nm (Fig. 6(b)), which correspond to the *c*-axis length of the unit cell and the thickness of a single molecule (LaO) or (CuSe) layer, respectively. The wide gap p-type degenerate conduction, the high-density hole doping, and the atomically flat surface make LaCuOSe:Mg a promising material for improved hole-injection electrodes in optoelectronic devices such as organic and inorganic LEDs.

2.4. Optical properties of $LaCuOS_{1-x}Se_x$ ($x = 0$–1) epitaxial films[52]

Fig. 7 shows the PL and absorption spectra of the LaCuOS and LaCuOSe epitaxial films at 10 K. A sharp excitonic absorption peak is observed at 3.280 eV for LaCuOS. On the other hand, two absorption peaks at 3.085 and 2.960 eV are observed for LaCuOSe. This energy splitting of $\sim$125 meV originates from the spin–orbit interaction in the Se ions.[19] Due to the high-quality of the films, the sharp PL bands peaking at 3.241 eV for LaCuOS and 2.925 eV for LaCuOSe are clearly observed near the band edge. These PL peaks are attributed to bound excitons. The full widths at half maximum of the bound-excitonic PL

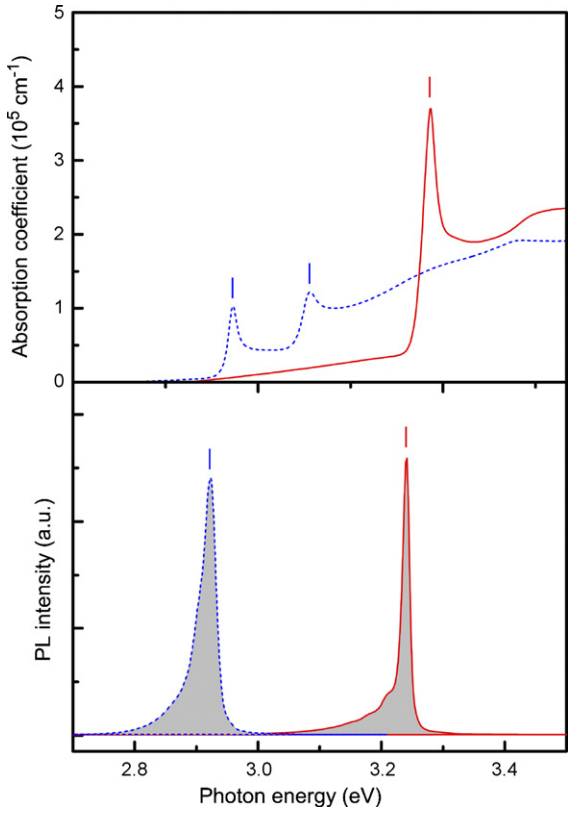

Fig. 7. Optical absorption and PL spectra of LaCuOS (solid line) and LaCuOSe (dotted lines) epitaxial films at 10 K. The excitation source of the PL spectra is a He–Cd laser ($\lambda = 325$ nm, excitation density = ~30 mW cm^{-2}).

bands are ~10 meV for LaCuOS and ~30 meV for LaCuOSe, respectively.

Fig. 8 shows the PL energies in $LaCuOS_{1-x}Se_x$ ($x = 0$–1) epitaxial films at room temperature as a function of Se content x. The emission energy decreases almost linearly as the x increases, which allows one to tune the emission energy from 3.21 eV (386 nm) to 2.89 eV (429 nm) by changing x. The decrease in the emission energy is attributed to a change in the VBM electronic structure because the VB dispersion is increased and consequently the band gap is decreased when more Se ions substitute for the S ions. The controllability of the emission wavelength (from 386 to 429 nm) and the electrical conductivity (from a thermally-activated type to a metallic conduction) in LaCuO*Ch* are promising properties for an emitting layer in light-emitting devices as well as a transparent hole-injection layer.

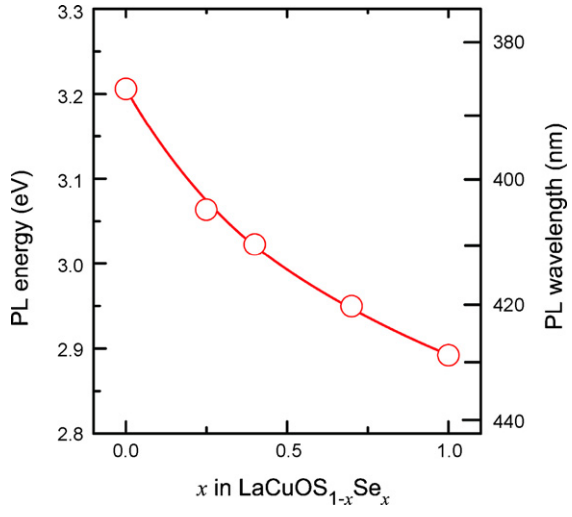

Fig. 8. PL energies of $LaCuOS_{1-x}Se_x$ ($x = 0$–1) epitaxial films at room temperature as a function of Se content x.

2.5. *Blue LED based on LaCuOSe epitaxial film*[53]

The efficient blue PL due to the room-temperature stable exciton and the controllable p-type conductivity make LaCuO*Ch*, especially LaCuOSe, promising materials for optoelectronic devices that operate in the short wavelength region. A drawback of these oxychalcogenides is the difficulty in obtaining an isostructural n-type layer, making it impossible to fabricate a pn homo-junction. Therefore, we fabricated a pn hetero-junction by depositing an n-type amorphous indium gallium zinc oxide [a-$InGaZn_5O_8$, the band gap is ~3.5 eV] layer[54–56] on a p-type epitaxial LaCuOSe film. The essential merit of the employment of an amorphous material as a n-type layer is the capability of low temperature fabrication of pn junction which prevent serious degradation of the hetero-interface due, e.g., to thermal diffusion.

Fig. 9 shows the electroluminescence (EL) spectra of the pn hetero-junction measured at room temperature as a function of injected current density. A sharp blue EL band at $\lambda = $ ~430 nm first appears at a forward current density ($I_{forward}$) of ~1.4 A cm^{-2}. The intensity increases with $I_{forward}$ and tends to saturate with a further increase in $I_{forward}$. It is confirmed that the energy and bandwidth of the EL spectra agree well with those of the PL spectrum. That is, the electrons injected from the a-$InGaZn_5O_8$ layer are coupled with the holes in the p-type LaCuOSe layer to form the excitons, which are annihilated by emitting blue luminescence. This is the first demonstration of an excitonic LED composed of the oxychalcogenides.

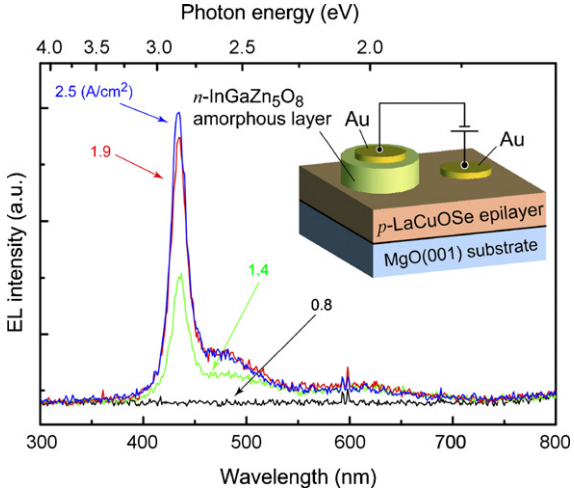

Fig. 9. EL spectra of a pn hetero-junction LED composed of p-LaCuOSe epilayer and n-$InGaZn_5O_8$ amorphous layer, measured from the MgO substrate at room temperature as a function of the current density. The inset shows the device structure.

3. Oxypnictide, LaT_MOPn (T_M = 3d transition metal, Pn = pnicogen)

3.1. Novel Fe-based superconductor, LaFeOP[57]

Systematic research on layered oxychalcogenides, LaCuOCh (Ch = chalcogen),[6,58] has implied that the (CuCh) layer, which is sandwiched by the larger energy gap (LaO) oxide layers, works as a hole carrier transport path. As an analog, the ($T_M Pn$) layer in an isostructural compound LaT_MOPn is also expected to be a carrier conduction layer sandwiched by the (LaO) larger energy gap layers as shown in Fig. 1. This two-dimensional crystal structure, which contains a 3d transition metal ion, led to the expectation that interesting electronic and/or magnetic properties would be discovered based on the electron correlation. Consequently, we found a novel superconductor in the Fe-based layered system, LaFeOP.

Fig. 10 shows the temperature dependence of electrical resistivity (ρ) of undoped and F-doped LaOFeP polycrystalline bulks, synthesized by a solid-state reaction. Both the data exhibit metallic behavior at temperatures >10 K (inset of Fig. 10). At temperatures below 5 K, a sharp drop in ρ for undoped LaFeOP is observed, and the resistivity vanishes at 3.2 K, implying the transition to a superconductivity phase. The superconducting transition temperature is significantly raised by F-doping. The transition temperature shifts to lower temperatures with increasing a magnetic field (H), indicating that the magnetic field breaks the superconductivity state (Fig. 11(a)). The magnetic susceptibilities (χ) measured in zero-field cooling processes (Fig. 11(b)) reach -2.4×10^{-3} emu/g and -1.2×10^{-2} emu/g at 2.3 K for undoped and F-doped LaFeOP, respectively. These values correspond to the volume fractions of the superconductivity phase of 18% and 91%, respectively. These observations, i.e., the zero resistivity and the perfect diamagnetism, verify the occurrence of the superconducting transition in LaFeOP at ~4 K. A magnetization curve showed a typical profile for a type-II superconductor similar to layered copper-based oxides, and the lower superconducting critical magnetic field (H_{c1}) was observed at ~17 Oe and the upper superconducting critical magnetic field (H_{c2}) at >1000 Oe.

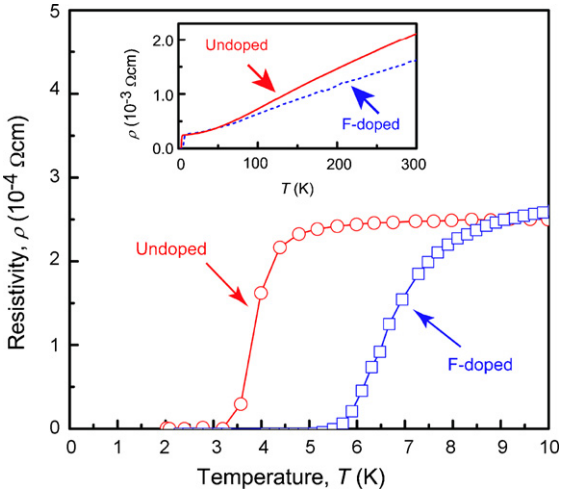

Fig. 10. Temperature dependence of electrical resistivity of undoped (circles) and F-doped (squares) LaFeOP at 0 Oe. The inset shows an expanded view from ~1.8 to 300 K.

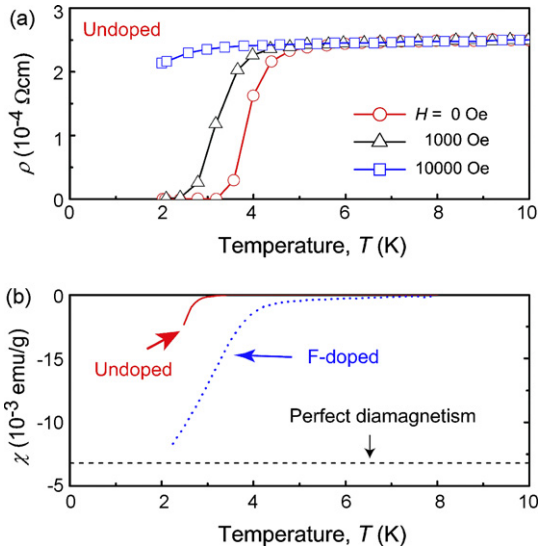

Fig. 11. (a) Temperature dependence of electrical resistivity (ρ) of undoped LaFeOP at various magnetic fields (H). (b) Temperature dependence of magnetic susceptibility (χ) of undoped (solid line) and F-doped (dotted line) LaFeOP. The horizontal dashed line shows the χ value of the perfect diamagnetism.

There is a distinct difference in the coordination structure in LaFeOP compared with the layered copper-based superconductors reported so far; that is, a Cu^{2+} ion in the layered copper-based superconductors occupies a planar fourfold square site while Fe^{2+} in LaOFeP occupies a tetrahedral site coordinated with four P^{3-} ions, and the tetrahedrons are linked with each other by edge-sharing to form the (FeP) layer, as shown in Fig. 1(b). As a consequence, the electrons at the Fermi level occupy Cu^{2+} $3d_{x2-y2}$ orbitals in the layered copper-based superconductors, while Fe^{2+} $3d_{z2}$ and $3d_{xz, yz}$ orbitals form the Fermi level for LaFeOP. These features suggest that LaFeOP has an importance for superconductivity physics and material exploration: the finding of the new iron-based superconductor with a different type of a layered structure will provide an opportunity for studying the mechanism of high-T_c superconductivity in layered crystals.

3.2. Superconducting properties of LaNiOP[59]

Since the finding of superconductivity in LaFeOP, we have extended the material system to other LaT_MOPn with other T_M such as Mn ($3d^5$) and Co ($3d^7$) and have found that LaMnOP[60] and LaCoOP[61] are, respectively, an antiferromagnetic semiconductor and a ferromagnetic metal. That is, electrical and magnetic properties of this oxypnictide series drastically change by varying T_M ions. Next, we were therefore interested in electrical and magnetic properties of an isostructural compound LaNiOP, in which Ni has an electronic configuration of $3d^8$. However, synthesis of LaNiOP was not reported previously. Recently, we succeeded in preparing LaNiOP polycrystalline bulk sample by a solid-state reaction using a stoichiometric

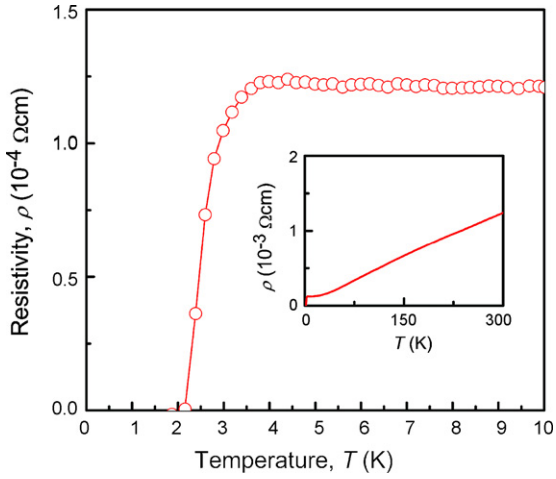

Fig. 12. Temperature dependence of electrical resistivity of LaNiOP at 0 Oe. The inset shows an expanded view from ~1.8 to 300 K.

mixture of LaP and NiO, and found that LaNiOP was also a superconductor.

Fig. 12 shows the temperature dependence of the electrical resistivity at $H = 0$ Oe. The resistivity exhibits a metallic behavior, begins to drop around 4 K, and becomes zero around 2 K. The onset temperature shifts to a lower temperature as the H increases, and the drop in ρ vanishes at $H = 10{,}000$ Oe (Fig. 13). These results suggest that the obtained LaNiOP exhibits a superconducting transition at ~3 K. The temperature dependence of the magnetic susceptibility (χ) implies a Pauli paramagnetism between 4 and 300 K as shown in the inset of Fig. 13. However, χ begins to drop and becomes negative at ~3 K. It reaches a large negative value of -5.3×10^{-3} emu/g at 1.8 K. These results, together with the zero resistance, clearly indicate that LaNiOP exhibits superconductivity at temperatures below 4 K. The volume fraction of the superconducting phase estimated from the χ value at 1.8 K is ~40 vol.%. From the magnetization curve, we have clarified that LaNiOP is a type II superconductor, like LaFeOP, with lower and upper critical magnetic fields of $H_{c1} = \sim 20$ Oe and $H_{c2} = \sim 800$ Oe, respectively.

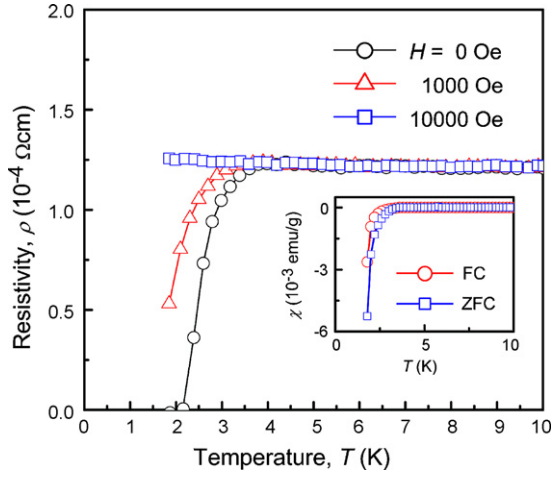

Fig. 13. Temperature dependence of electrical resistivity of LaNiOP at various magnetic fields (H). The inset shows temperature dependence of magnetic susceptibility (χ) of LaNiOP, measured under conditions of zero-field cooling (ZFC) and filed cooling (FC) at $H_{FC} = 10$ Oe.

4. Summary and concluding remarks

Characteristic properties in mixed-anion layered compounds such as oxychalcogenide LaCuO*Ch* (*Ch* = chalcogen) and oxypnictide LaT_MO*Pn* (T_M = 3d transition metal, *Pn* = pnicogen) were reviewed with an emphasis on the two-dimensional structure. Successful fabrication of epitaxial thin films of LaCuO*Ch* with the reactive solid-phase epitaxy (R-SPE) is a key to discovering unique optoelectronic properties and demonstrating a room-temperature operation of light-emitting diode (LED) using LaCuOSe. Furthermore, novel superconductors LaT_MOP (T_M = Fe and Ni) have been found by extending the material system from oxychalcogenides to oxypnictides. The useful and/or applicable properties found for this material series are summarized as follow:

(1) The high hole mobility of 8.0 $cm^2/(V\,s)$ is obtained for undoped LaCuOSe epitaxial film.
(2) Heavy hole doping $>10^{21}$ cm^{-3} is attained in Mg-doped LaCuOSe epitaxial films. The conductivity reaches 910 S cm^{-1} ($\rho = 1.1 \times 10^{-3}$ Ω cm).
(3) High efficient photoluminescence from room-temperature stable excitons is observed. The peak position is tunable from 386 to 429 nm by changing the *Ch* composition.
(4) Blue LEDs based on LaCuOSe epilayers operate at room temperature and emit excitonic sharp luminescence.
(5) Novel layered superconductors were found in oxypnictides, LaT_MOP (T_M = Fe and Ni). These findings lead to a very recent discovery of a new superconductor with a high T_c of 26 K, F-doped LaFeOAs.[62]

These unique properties originate from low-dimensional electronic structures due to the sandwiched structures composed of narrow-gap Cu*Ch*/T_M*Pn* layers and larger-gap (LaO) layers. We may anticipate, therefore, this type of a layered material, which is composed of atomic layers with different energy gaps, is a promising material for optoelectronic/magnetic applications.

References

1. Ueda, K., Inoue, S., Hirose, S., Kawazoe, H. and Hosono, H., Transparent p-type semiconductor: LaCuOS layered oxysulfide. *Appl. Phys. Lett.*, 2000, **77**, 2701–2703.
2. Ueda, K. and Hosono, H., Band gap engineering, band edge emission, and p-type conductivity in wide-gap $LaCuOS_{1-x}Se_x$ oxychalcogenides. *J. Appl. Phys.*, 2002, **91**, 4768–4770.
3. Ueda, K., Takafuji, K., Hiramatsu, H., Ohta, H., Kamiya, T., Hirano, M. and Hosono, H., Electrical and optical properties and electronic structures of LnCuOS (Ln = La~Nd). *Chem. Mater.*, 2003, **15**, 3692–3695.
4. Kawazoe, H., Yasukawa, M., Hyodo, H., Kurita, M., Yanagi, H. and Hosono, H., P-type electrical conduction in transparent thin films of $CuAlO_2$. *Nature*, 1997, **389**, 939–942.
5. Kawazoe, H., Yanagi, H., Ueda, K. and Hosono, H., Transparent p-type conducting oxides: design and fabrication of p–n heterojunctions. *MRS Bull.*, 2000, **25**, 28–36.

6. Ueda, K., Hiramatsu, H., Hirano, M., Kamiya, T. and Hosono, H., Wide-gap layered oxychalcogenide semiconductors: materials, electronic structures and optoelectronic properties. *Thin Solid Films*, 2006, **496**, 8–15.
7. Palazzi, M., Préparation et affinement de la structure de (LaO)CuS. *C.R. Acad. Sci. (Paris)*, 1981, **292**, 789–791.
8. Zhu, W. J., Huang, Y. Z., Dong, C. and Zhao, Z. X., Synthesis and crystal structure of new rare-earth copper oxyselenides: RCuSeO (R = La, Sm, Gd and Y). *Mater. Res. Bull.*, 1994, **29**, 143–147.
9. Popovkin, B. A., Kusainova, A. M., Dolgikh, V. A. and Aksel'rud, L. G., New layered phases of the MOCu*X* (M = Ln, Bi; *X* = S, Se, Te) family: a geometric approach to the explanation of phase stability. *Russ. J. Inorg. Chem.*, 1998, **43**, 1471–1475.
10. Charkin, D. O., Akopyan, A. V. and Dolgikh, V. A., New mixed rare-earth copper oxochalcogenides with a LaOAgS-type structure. *Russ. J. Inorg. Chem.*, 1999, **44**, 833–837.
11. Charkin, D. O., Berdonosov, P. S., Dolgikh, V. A. and Lightfoot, P., New lanthanide–silver oxochalcogenides with a LaOAgS-type structure: crystal-chemical boundaries of the existence of this structural type. *Russ. J. Inorg. Chem.*, 2000, **45**, 182–189.
12. Takase, K., Sato, K., Shoji, O., Takahashi, Y., Takano, Y., Sekizawa, K., Kuroiwa, Y. and Goto, M., Charge density distribution of transparent p-type semiconductor (LaO)CuS. *Appl. Phys. Lett.*, 2007, **90**, 161916.
13. Inoue, S., Ueda, K., Hosono, H. and Hamada, N., Electronic structure of the transparent p-type semiconductor (LaO)CuS. *Phys. Rev. B*, 2001, **64**, 245211.
14. Sato, H., Negishi, H., Wada, A., Ino, A., Negishi, S., Hirai, C., Namatame, H., Taniguchi, M., Takase, K., Takahashi, Y., Shimizu, T., Takano, Y. and Sekizawa, K., Electronic structure of oxysulfide (LaO)CuS and $(La_{1-x}Ca_xO)Cu_{1-x}Ni_xS$ ($x < \sim 0.10$) studied by photoemission and inverse-photoemission spectroscopies. *Phys. Rev. B*, 2003, **68**, 035112.
15. Ueda, K., Hosono, H. and Hamada, N., Energy band structure of LaCuOCh (Ch = S, Se and Te) calculated by the full-potential linearized augmented plane-wave method. *J. Phys., Condens. Matter*, 2004, **16**, 5179–5186.
16. Kamiya, T., Ueda, K., Hiramatsu, H., Kamioka, H., Ohta, H., Hirano, M. and Hosono, H., Two-dimensional electronic structure and multiple excitonic states in layered oxychalcogenide semiconductors, LaCuOCh (Ch = S, Se, Te): optical properties and relativistic ab initio study. *Thin Solid Films*, 2005, **486**, 98–103.
17. Ueda, K., Hosono, H. and Hamada, N., Valence-band structures of layered oxychalcogenides, LaCuOCh (Ch = S, Se, and Te), studied by ultraviolet photoemission spectroscopy and energy-band calculations. *J. Appl. Phys.*, 2005, **98**, 043506.
18. Yanagi, H., Tate, J., Park, S., Park, C.-H., Keszler, D. A., Hirano, M. and Hosono, H., Valence band structure of BaCuSF and BaCuSeF. *J. Appl. Phys.*, 2006, **100**, 083705.
19. Ueda, K., Hiramatsu, H., Ohta, H., Hirano, M., Kamiya, T. and Hosono, H., Single-atomic-layered quantum wells built in wide-gap semiconductors *Ln*CuO*Ch* (*Ln* = lanthanide, *Ch* = chalcogen). *Phys. Rev. B*, 2004, **69**, 155305.
20. Ueda, K., Inoue, S., Hosono, H., Sarukura, N. and Hirano, M., Room-temperature excitons in wide-gap layered-oxysulfide semiconductor: LaCuOS. *Appl. Phys. Lett.*, 2001, **78**, 2333–2335.
21. Kamioka, H., Hiramatsu, H., Ohta, H., Hirano, M., Ueda, K., Kamiya, T. and Hosono, H., Third-order optical nonlinearity originating from room-temperature exciton in layered compounds LaCuOS and LaCuOSe. *Appl. Phys. Lett.*, 2004, **84**, 879–881.
22. Zimmer, B. I., Jeitschko, W., Albering, J. H., Glaum, R. and Reehuis, M., The rare earth transition metal phosphide oxides LnFePO, LnRuPO and LnCoPO with ZrCuSiAs type structure. *J. Alloy Compd.*, 1995, **229**, 238–242.
23. Nientiedt, A. T., Jeitschko, W., Pollmeier, P. G. and Brylak, M., Quaternary equiatomic manganese pnictide oxides AMnPO (A = La–Nd, Sm, Gd–Dy), AMnAsO (A = Y, La–Nd, Sm, Gd–Dy, U), and AMnSbO (A = La–Nd, Sm, Gd) with ZrCuSiAs type structure. *Z. Naturforsch.*, 1997, **52b**, 560–564.
24. Nientiedt, A. T. and Jeitschko, W., Equiatomic quaternary rare earth element zinc pnictide oxides RZnPO and RZnAsO. *Inorg. Chem.*, 1998, **37**, 386–389.
25. Charkin, D. O., Berdonosov, P. S., Dolgikh, V. A. and Lightfoot, P., Novel lanthanoid–cadmium oxide pnictides with the tetragonal LaOAgS structure. *J. Alloy Compd.*, 1999, **292**, 118–123.
26. Hiramatsu, H., Ueda, K., Ohta, H., Orita, M., Hirano, M. and Hosono, H., Heteroepitaxial growth of a wide-gap p-type semiconductor, LaCuOS. *Appl. Phys. Lett.*, 2002, **81**, 598–600.
27. Hiramatsu, H., Ueda, K., Takafuji, K., Ohta, H., Hirano, M., Kamiya, T. and Hosono, H., Fabrication of heteroepitaxial thin films of layered oxychalcogenides LnCuOCh (Ln = La–Nd; Ch = S–Te) by reactive solid-phase epitaxy. *J. Mater. Res.*, 2004, **19**, 2137–2143.
28. Ohta, H., Nomura, K., Orita, M., Hirano, M., Ueda, K., Suzuki, T., Ikuhara, Y. and Hosono, H., Single-crystalline films of the homologous series $InGaO_3(ZnO)_m$ grown by reactive solid-phase epitaxy. *Adv. Funct. Mater.*, 2003, **13**, 139–144.
29. Nomura, K., Ohta, H., Ueda, K., Orita, M., Hirano, M. and Hosono, H., Novel film growth technique of single crystalline $In_2O_3(ZnO)_m$ (m = integer) homologous compound. *Thin Solid Films*, 2002, **411**, 147–151.
30. Nomura, K., Ohta, H., Ueda, K., Kamiya, T., Hirano, M. and Hosono, H., Thin-film transistor fabricated in single-crystalline transparent oxide semiconductor. *Science*, 2003, **300**, 1269–1272.
31. Nomura, K., Ohta, H., Ueda, K., Kamiya, T., Orita, M., Hirano, M., Suzuki, T., Honjyo, C., Ikuhara, Y. and Hosono, H., Growth mechanism for single-crystalline thin film of $InGaO_3(ZnO)_5$ by reactive solid-phase epitaxy. *J. Appl. Phys.*, 2004, **95**, 5532–5539.
32. Hiramatsu, H., Ueda, K., Kamiya, T., Ohta, H., Hirano, M. and Hosono, H., Optical properties and two-dimensional electronic structure in wide-gap layered oxychalcogenide: $La_2CdO_2Se_2$. *J. Phys. Chem. B*, 2004, **108**, 17344–17351.
33. Nomura, K., Ohta, H., Ueda, K., Kamiya, T., Hirano, M. and Hosono, H., All oxide transparent MISFET using high-*k* dielectrics gates. *Microelectron. Eng.*, 2004, **72**, 294–298.
34. Kamioka, H., Hiramatsu, H., Hirano, M., Ueda, K., Kamiya, T. and Hosono, H., Quantum beat between two excitonic levels split by spin–orbit interactions in the oxychalcogenide LaCuOS. *Opt. Lett.*, 2004, **29**, 1659–1661.
35. Nomura, K., Kamiya, T., Ohta, H., Ueda, K., Hirano, M. and Hosono, H., Carrier transport in transparent oxide semiconductor with intrinsic structural randomness probed using single-crystalline $InGaO_3(ZnO)_5$ films. *Appl. Phys. Lett.*, 2004, **85**, 1993–1995.
36. Ohta, H., Kim, S.-W., Ohta, S., Koumoto, K., Hirano, M. and Hosono, H., Reactive solid-phase epitaxial growth of Na_xCoO_2 ($x \sim 0.83$) via lateral diffusion of Na into a cobalt oxide epitaxial layer. *Cryst. Growth Des.*, 2005, **5**, 25–28.
37. Sugiura, K., Ohta, H., Nomura, K., Yanagi, H., Hirano, M., Hosono, H. and Koumoto, K., Epitaxial film growth and superconducting behavior of sodium–cobalt oxyhydrate, $Na_xCoO_2{\cdot}yH_2O$ ($x \sim 0.3$, $y \sim 1.3$). *Inorg. Chem.*, 2006, **45**, 1894–1896.
38. Ogo, Y., Nomura, K., Yanagi, H., Ohta, H., Kamiya, T., Hirano, M. and Hosono, H., Growth and structure of heteroepitaxial thin films of homologous compounds $RAO_3(MO)_m$ by reactive solid-phase epitaxy: applicability to a variety of materials and epitaxial template layers. *Thin Solid Films*, 2006, **496**, 64–69.
39. Sugiura, K., Ohta, H., Nomura, K., Hirano, M., Hosono, H. and Koumoto, K., Fabrication and thermoelectric properties of layered cobaltite, γ-$Sr_{0.32}Na_{0.21}CoO_2$ epitaxial films. *Appl. Phys. Lett.*, 2006, **88**, 082109.
40. Kamiya, T., Takeda, Y., Nomura, K., Ohta, H., Yanagi, H., Hirano, M. and Hosono, H., Self-adjusted, three-dimensional lattice-matched buffer layer for growing ZnO epitaxial film: homologous series layered oxide, $InGaO_3(ZnO)_5$. *Cryst. Growth Des.*, 2006, **6**, 2451–2456.
41. Sugiura, K., Ohta, H., Nomura, K., Hirano, M., Hosono, H. and Koumoto, K., High electrical conductivity of layered cobalt oxide $Ca_3Co_4O_9$ epitaxial films grown by topotactic ion-exchange method. *Appl. Phys. Lett.*, 2006, **89**, 032111.
42. Kayanuma, K., Kawamura, R., Hiramatsu, H., Yanagi, H., Hirano, M., Kamiya, T. and Hosono, H., Heteroepitaxial growth of layered semiconductors, LaZnOPn (P*n* = P and As). *Thin Solid Films*, 2008, doi:10.1016/j.tsf.2007.10.035, (online).
43. Hiramatsu, H., Ohta, H., Suzuki, T., Honjo, C., Ikuhara, Y., Ueda, K., Kamiya, T., Hirano, M. and Hosono, H., Mechanism for heteroepitaxial growth of transparent p-type semiconductor: LaCuOS by reactive solid-phase epitaxy. *Cryst. Growth Des.*, 2004, **4**, 301–307.

44. Hiramatsu, H., Ueda, K., Ohta, H., Hirano, M., Kamiya, T. and Hosono, H., Degenerate p-type conductivity in wide-gap $LaCuOS_{1-x}Se_x$ ($x = 0$–1) epitaxial films. *Appl. Phys. Lett.*, 2003, **82**, 1048–1050.
45. Hiramatsu, H., Ueda, K., Takafuji, K., Ohta, H., Hirano, M., Kamiya, T. and Hosono, H., Degenerate electrical conductive and excitonic photoluminescence properties of epitaxial films of wide gap p-type layered oxychalcogenides, LnCuOCh (Ln = La, Pr and Nd; Ch = S or Se). *Appl. Phys. A*, 2004, **79**, 1521–1523.
46. Amano, H., Kito, M., Hiramatsu, K. and Akasaki, I., P-type conduction in Mg-doped GaN treated with low-energy electron beam irradiation (LEEBI). *Jpn. J. Appl. Phys.*, 1989, **28**, L2112–L2114.
47. Nakamura, S., Mukai, T., Senoh, M. and Iwasa, N., Thermal annealing effects on p-type Mg-doped GaN films. *Jpn. J. Appl. Phys.*, 1992, **31**, L139–L142.
48. Akasaki, I. and Amano, H., Crystal growth and conductivity control of group III nitride semiconductors and their application to short wavelength light emitters. *Jpn. J. Appl. Phys.*, 1997, **36**, 5393–5408.
49. Hiramatsu, H., Ueda, K., Ohta, H., Hirano, M., Kikuchi, M., Yanagi, H., Kamiya, T. and Hosono, H., Heavy hole doping of epitaxial thin films of a widegap p-type semiconductor, LaCuOSe, and analysis of the effective mass. *Appl. Phys. Lett.*, 2007, **91**, 012104.
50. Tsukazaki, A., Ohtomo, A., Onuma, T., Ohtani, M., Makino, T., Sumiya, M., Ohtani, K., Chichibu, S. F., Fuke, S., Segawa, Y., Ohno, H., Koinuma, H. and Kawasaki, M., Repeated temperature modulation epitaxy for p-type doping and light-emitting diode based on ZnO. *Nat. Mater.*, 2005, **4**, 42–46.
51. Hiramatsu, H., Ueda, K., Ohta, H., Hirano, M. and Hosono, H., Heteroepitaxial growth of a wide gap p-type oxysulfide, LaCuOS. *Mater. Res. Soc. Symp. Proc.*, 2003, **747**, 359–364.
52. Hiramatsu, H., Ueda, K., Takafuji, K., Ohta, H., Hirano, M., Kamiya, T. and Hosono, H., Intrinsic excitonic photoluminescence and band-gap engineering of wide-gap p-type oxychalcogenide epitaxial films of LnCuOCh (Ln = La, Pr, and Nd; Ch = S or Se) semiconductor alloys. *J. Appl. Phys.*, 2003, **94**, 5805–5808.
53. Hiramatsu, H., Ueda, K., Ohta, H., Kamiya, T., Hirano, M. and Hosono, H., Excitonic blue luminescence from p-LaCuOSe/n-$InGaZn_5O_8$ light-emitting diode at room temperature. *Appl. Phys. Lett.*, 2005, **87**, 211107.
54. Orita, M., Ohta, H., Hirano, M., Narushima, S. and Hosono, H., Amorphous transparent conductive oxide $InGaO_3(ZnO)_m$ ($m \leq 4$): A Zn 4s conductor. *Philos. Mag. B*, 2001, **81**, 501–515.
55. Nomura, K., Ohta, H., Takagi, A., Kamiya, T., Hirano, M. and Hosono, H., Room-temperature fabrication of transparent flexible thin-film transistors using amorphous oxide semiconductors. *Nature*, 2004, **432**, 488–492.
56. Hosono, H., Ionic amorphous oxide semiconductors: material design, carrier transport, and device application. *J. Non-Cryst. Solids*, 2006, **352**, 851–858.
57. Kamihara, Y., Hiramatsu, H., Hirano, M., Kawamura, R., Yanagi, H., Kamiya, T. and Hosono, H., Iron-based layered superconductor: LaOFeP. *J. Am. Chem. Soc.*, 2006, **128**, 10012–10013.
58. Hiramatsu, H., Kamioka, H., Ueda, K., Ohta, H., Kamiya, T., Hirano, M. and Hosono, H., Opto-electronic properties and light-emitting device application of widegap layered oxychalcogenides: LaCuO*Ch* (*Ch* = chalcogen) and $La_2CdO_2Se_2$. *Phys. Stat. Sol. A*, 2006, **203**, 2800–2811.
59. Watanabe, T., Yanagi, H., Kamiya, T., Kamihara, Y., Hiramatsu, H., Hirano, M. and Hosono, H., Nickel-based oxyphosphide superconductor with a layered crystal structure, LaNiOP. *Inorg. Chem.*, 2007, **46**, 7719–7721.
60. Yanagi, H., *et al.*, in preparation.
61. Yanagi, H., Kawamura, R., Kamiya, T., Kamihara, Y., Hirano, M., Nakamura, T., Osawa, H., and Hosono, H. Itinerant ferromagnetism in layered crystals LaCoO*Pn* (*Pn* = P, As), submitted for publication.
62. Kamihara, Y., Watanabe, T., Hirano, M. and Hosono, H., Iron-based layered superconductor $La[O_{1-x}F_x]FeAs$ ($x = 0.05$–0.12) with $T_c = 26$ K. *J. Am. Chem. Soc.*, 2008, **130**, 3296–3297.